Electron Parametric Instabilities Driven by Relativistically Intense Laser Light in Plasma

H. C. Barr, P. Mason, and D. M. Parr
Department of Physics, University of Essex, Colchester CO4 3SQ, England
(Received 24 February 1999)

A unified treatment of electron parametric instabilities driven by ultraintense laser light in plasma is described. It is valid for any intensity, polarization, plasma density, and scattering geometry. The method is applied to linearly polarized light in both underdense plasma and overdense plasma accessible by self-induced transparency. New options arise which are hybrids of stimulated Raman scattering, the two plasmon decay, the relativistic modulational and filamentation instabilities, and stimulated harmonic generation. There is vigorous growth over a wide range of wave numbers and harmonics.

PACS numbers: 52.40.Nk, 52.25.Rv, 52.35.Mw

The high fields attained in current laser pulses produce novel effects in plasmas which are of fundamental and practical interest [1,2]. In particular, vigorous parametric instabilities are driven which can rapidly degrade and deplete intense pulses. At intensities where electrons quiver with relativistic velocities, new regimes of purely electronic parametric instabilities, not evident at lower intensities, appear. Their understanding is basic to the success of applications such as the fast ignition of laser fusion targets [3], plasma-based electron accelerator schemes [4], and many others.

At nonrelativistic intensities, the dominant electron parametric instabilities are stimulated Raman scattering (SRS) at densities up to the quarter critical density $n_c/4$ (n_c, the laser critical density) and the two plasmon decay (TPD) instability at $n_c/4$ [5,6]. Oscillations in the relativistic electron mass give rise to the relativistic modulational instability (RMI) when the modulation is in the laser propagation direction or the relativistic filamentation instability (RFI) when it is transverse [7]. At ultrahigh intensities where the normalized vector potential $a_0 > 1$ [$a_0 = eA_0/mc^2 = 0.85 \times 10^{-9}\lambda(\mu\mathrm{m})I^{1/2}(\mathrm{W/cm^2})$, I is the intensity, and λ the laser wavelength], these are accompanied by stimulated harmonic generation by a higher order Raman scattering process which emerges strongly to give a rich tableau of parametric instabilities. So far, the extension of theory to ultrahigh intensities has not been practical in generality. It has not been possible to cater for the harmonic content in linearly polarized laser drivers, to deal with instability self-consistently for all accessible densities, nor usually to go beyond a three or four wave theory. In addition, existing descriptions have relied on one or more of various restrictions and assumptions: circular polarization, underdense plasma, weak relativity, the quasistatic, WKB or paraxial approximations, or limitation to 1D models of back and forward scattering [8–14]. None of these are used in the work described here.

In this Letter, we present a general approach which, for the first time, obtains the characteristics of all purely electronic parametric instabilities. The method is valid (i) at ultrahigh laser intensity, (ii) for any laser polarization and, in particular, for linear polarization where the electron dynamics are nonlinear, (iii) for both under and overdense plasmas (where the transparency is laser self-induced by the relativistic mass increase), and (iv) for any scattering geometry, i.e., it is fully three dimensional. A large amplitude plane light wave, the laser driver, propagating in a plasma at a phase velocity v_p adopts an anharmonic waveform (circular polarization is the exception) which may be expressed as a superposition of harmonics $(l\omega_0, l\mathbf{k}_0 = lk_0\hat{\mathbf{x}})$, where l is any integer, ω_0 (k_0) is the fundamental frequency (wave number), and $v_p = \omega_0/k_0$. The dispersion relation is $\omega_0^2 = \Omega_0^2 + k_0^2c^2$, where Ω_0 is the plasma frequency at low intensities but is otherwise a complex function of density and laser intensity. Such laser light couples a fluctuation at $(\omega, \mathbf{k})$ to sidebands at $(\omega + l\omega_0, \mathbf{k} + l\mathbf{k}_0)$ [5]. If any pair of these corresponds to a resonant electron plasma wave at $\omega = \omega_p$ (the plasma frequency) and a resonant Nth harmonic electromagnetic wave at $\omega_s = N\omega_0 - \omega$, then parametric instability is possible. We refer to this as stimulated Raman harmonic generation (SRHG). At low intensities ($a_0 < 1$), stimulated Raman scattering ($N = 1$) dominates over higher order harmonic generation. If the decay is into adjacent modes which are both plasma waves then this is the TPD instability. A second order TPD process is possible at n_c but other higher order TPD options cannot occur. Instability also arises due to zero-order oscillations or first-order fluctuations in the electron mass increase as in the RMI and RFI instabilities. Higher order versions of these also occur. At ultrahigh intensities ($a_0 > 1$), many Fourier modes become strongly coupled and higher order processes attain growth rates comparable with SRS, TPD, RMI, and RFI. Indeed, overlap and interference between these produce parametric instabilities which are hybrids of stimulated Raman harmonic generation, the two plasmon decay, and modulational instabilities.

A covariant formulation of a cold electron fluid plasma is adopted in which the choice of frame is central. Assume a frame moving with velocity $\mathbf{u} = u\hat{\mathbf{x}}$ relative to the laboratory frame so that the ambient electrons and ions flow with velocity $-\mathbf{u}$. The momentum equation is

$$\frac{\partial}{\partial t}(\mathbf{p} - \mathbf{A}) = \nabla(\phi - \gamma), \tag{1}$$

 0031-9007/99/83(8)/1606(4)$15.00

where $\mathbf{p}$ is the electron momentum, $\mathbf{A}$ (ϕ) the vector (scalar) potential, and $\gamma = (1 + p^2)^{1/2}$. Times are normalized to ω_0^{-1}, velocities to c, lengths to c/ω_0, and $\mathbf{p}/mc \to \mathbf{p}$, $e\mathbf{A}/mc^2 \to \mathbf{A}$, and $e\phi/mc^2 \to \phi$. The cold plasma assumption is justified at ultrahigh intensities, where the coherent electron velocity induced by the laser dominates any thermal motion. Equation (1) assumes that $\nabla \times (\mathbf{p} - \mathbf{A}) = 0$ initially and hence remains so. Expressing $\mathbf{p} - \mathbf{A} = \nabla\psi$ and integrating Eq. (1) we obtain

$$\frac{\partial \psi}{\partial t} = \phi - \gamma + \gamma_u , \tag{2}$$

where $\gamma_u = (1 - u^2)^{-1/2}$. Assuming the Coulomb gauge, Maxwell's equations take the form

$$\frac{\partial^2 \mathbf{A}}{\partial t^2} - \nabla^2 \mathbf{A} + \frac{n}{\gamma}\mathbf{A} = -\nabla \frac{\partial \phi}{\partial t} - \frac{n}{\gamma}\nabla\psi - n_0 \mathbf{u} , \tag{3}$$

$$\nabla^2 \phi = n - n_0 , \tag{4}$$

where the electron density n and ion density n_0 are normalized to $n_c = m\omega_0^2/4\pi e^2$.

The method is as follows. Monochromatic plane wave solutions are sought for the zero-order laser driver in the frame where the Poynting vector is zero. The frame moving at speed $u = 1/v_p$ achieves this. The wave then appears as a spatially homogeneous anharmonic oscillation in time at the frequency $\Omega_0 = 1/\gamma_u$. In effect, this is a Lorentz transformation to the laser group velocity frame, a natural choice for short pulses. In this "pulse" frame, the zero order is described by the spatially homogeneous form of Eqs. (1)–(4) so that $\mathbf{p}_0 = \mathbf{A}_0$, $n = n_0$, $\gamma_0 = (1 + p_0^2)^{1/2}$, and

$$\frac{d^2 \mathbf{p}_0}{dt^2} + \frac{n_0}{\gamma_0}\mathbf{p}_0 = -n_0 u \hat{\mathbf{x}} . \tag{5}$$

The periodic solution of Eq. (5) corresponding to the laser light is sought numerically to obtain $\mathbf{p}_0(t)$, $\gamma_0(t)$, and the period $2\pi/\Omega_0$. Equation (5) is equivalent to Eqs. (15) of Akhiezer and Polovin [15] who studied large amplitude laboratory frame solutions of Eqs. (2)–(4) depending only on the variable $x - v_p t$. It is the stability of this waveform which is now addressed.

The zero-order solution, being spatially homogeneous, implies no wave number coupling when the linearized equations are Fourier analyzed in space. Letting $\mathbf{b}_1 = i\mathbf{k} \times \mathbf{A}_1$ these are

$$\frac{d^2 \mathbf{b}_1}{dt^2} + [\omega_{\rm pr}^2(t) + k^2]\mathbf{b}_1 = ik\mathbf{c}_2(t)[k^2\phi_1 + \omega_{\rm pr}^2(t) \times (\phi_1 - d\psi_1/dt)], \tag{6}$$

$$\frac{d\phi_1}{dt} + \omega_{\rm pr}^2(t)\psi_1 = -ik^{-1}c_1(t)[k^2\phi_1 + \omega_{\rm pr}^2(t) \times (\phi_1 - d\psi_1/dt)], \tag{7}$$

$$\frac{d\psi_1}{dt} - \phi_1 = -ikc_1(t)\psi_1 + ik^{-1}\mathbf{c}_2(t)\cdot\mathbf{b}_1 , \tag{8}$$

where $c_1(t) = \hat{\mathbf{k}} \cdot \mathbf{v}_0(t)$, $\mathbf{c}_2(t) = \hat{\mathbf{k}} \times \mathbf{v}_0(t)$, $\mathbf{v}_0(t) = \mathbf{p}_0(t)/\gamma_0(t)$, and the relativistic plasma frequency $\omega_{\rm pr}(t) = [n_0/\gamma_0(t)]^{1/2}$. The right-hand sides of Eqs. (6) and (7) are proportional to $(n_1/n_0 - \gamma_1/\gamma_0)$, a combination of density fluctuations as in Raman scattering and relativistic mass fluctuations as in RMI and RFI. Instability can also result from the zero-order oscillations in $\omega_{\rm pr}(t)$. All contribute in varying measure at high intensity. The above system has the form $dy/dt = P_0(t)y$ with periodic coefficients $P_0(t)$ and so possesses Bloch (or Floquet) solutions $y = \exp(-i\omega t)P_1(t)$, where $P_1(t) = \sum_{l=-\infty}^{\infty} y_l \exp(-il\Omega_0 t)$ has the same period as $P_0(t)$. The periodic modulation of coefficients drives instability. The characteristic exponent $\omega = \Omega + i\Gamma$ is to be determined for the growth rate Γ and frequency shift Ω. For a given $\mathbf{k}$, we evolve Eqs. (6)–(8) in time for a few e foldings of the growth. This is sufficient to deduce Γ. Then Ω and the mode amplitudes y_l are extracted by Fourier analyzing the time signal after deconvolving the growth. If the growth rate is required in the laboratory rather than the pulse frame, an imaginary wave number $k_i = -u\Gamma$ is included, Γ obtained iteratively, and the 4-vector $(\omega, \mathbf{k})$ Lorentz transformed to the laboratory frame.

We now apply this approach to a linearly polarized driver. This is a coupled longitudinal-transverse wave [14] which, when viewed in the pulse frame, appears almost transverse. Take the plane of polarization to be the xy plane. First, define $\Omega_{\rm pr}^2 = n_{0,\rm lab}/\gamma_a$, where $\gamma_a = (1 + q^2/2)^{1/2}$, q the peak value of the transverse momentum p_{0y}, and $n_{0,\rm lab}$ the electron laboratory-frame density. Second, define a rms value for the relativistic plasma frequency $\omega_{\rm pr} = \langle \omega_{\rm pr}^2(t) \rangle^{1/2}$ where $\langle\,\rangle$ is an average over a laser period. The numerical solution of Eq. (5) shows that $\Omega_0 \approx \Omega_{\rm pr} \approx \omega_{\rm pr}$ at low intensities ($q < 1$) or at low densities ($u \approx 1$) even if $q > 1$. At high intensity in overdense plasma, these relationships still capture the main dependency on q; however, there are significant deviations. Let $\Omega_0 = \Omega_{\rm pr}/G(u, q)$ which is the pulse frame dispersion relation. $G(u, q)$ is a slowly varying function of the order of 1 such that $G(u, 0) = 1$ and varies between $G(u \approx 1, q) \approx 1$ and $G(u \approx 0, q \gg 1) \approx 2^{7/4}/\pi \approx 1.07$. The laser light cutoff ($u = 0$) occurs where $\Omega_{\rm pr} = G(0, q)$ so that the relativistic critical density $n_{\rm cr} = G^2(0, q)\gamma_a \approx 1.15\gamma_a$ when $q \gg 1$. This is a measure of the self-induced transparency. The laboratory-frame density is then $n_{0,\rm lab}/n_{\rm cr} = \gamma_u^{-2} G^2(u, q)/G^2(0, q) \sim \gamma_u^{-2}$. Equation (5) also shows that $\omega_{\rm pr} = \Omega_{\rm pr} H(u, q)$, where H is a slowly varying function of the order of 1. It satisfies $H(u, 0) = 1$ and varies from $H(u \approx 1, q) \approx 1$ to $H(u \approx 0, q = 100) \approx 1.5$.

The results below show the main regimes of growth categorized in terms of $n_{0,\rm lab}/n_{\rm cr}$ and the laser amplitude q. Low to moderate intensity ($q < 1$) regimes are dominated by the familiar SRS, TPD, RMI, and RFI instabilities adequately modeled by three and four wave theory. As the intensity becomes relativistic ($q = 1$–5), rapid growth

appears (i) at all densities, (ii) over wide regions of 3D wave number space, and (iii) at rates which can be a significant fraction of the laser frequency. At very relativistic intensities ($q > 5$) the coupling strength saturates ($|\mathbf{v}_0| \approx 1$) and growth rates then vary only weakly with q. Figures 1–3 are contour plots of the pulse-frame growth rate Γ/Ω_0 vs $\mathbf{K} = \mathbf{k}/\Omega_0$ when $q = 5$ showing typical patterns for underdense plasma, the relativistic quarter critical density, and the relativistic critical density. Significant growth extends to mode numbers well beyond those shown. In the absence of coupling but retaining the dc mass reduction of the plasma frequency [letting $\mathbf{v}_0 \rightarrow -u\hat{\mathbf{x}}$, $\omega_{\rm pr}(t) \rightarrow \omega_{\rm pr}$ in Eqs. (6)–(8)], the dispersion relation for light waves retains its invariant form $\omega^2 = \omega_{\rm pr}^2 + k^2$ and electron plasma waves have the Doppler-shifted time-dilated form $(\omega + k_x u)^2 = \omega_{\rm pr}^2/\gamma_u^2$. The dashed curves, included to guide the eye, correspond to exact 3-wave SRHG resonance between a scattered Nth harmonic $\omega_s = N\Omega - \omega$, where $\omega_s^2 = \omega_{\rm pr}^2 + k^2$ and a plasma wave $\omega = -k_x u + \omega_{\rm pr}/\gamma_u$. At high intensity, SRHG still has a dominant Fourier mode satisfying the light wave dispersion relation but, otherwise, there is a complex longitudinal-transverse multimode composition to each normal mode. SRHG at the Nth harmonic requires inclusion of $2(N + 2)$ modes to give a correct measure of the growth rate. Pure filamentation ($k_x = 0$) is seen to grow strongly on transverse scales $|\mathbf{k}_\perp| \approx \omega_{\rm pr}$ at rates not much less than that for the resonant SRHG processes.

Figure 1 illustrates the underdense plasma case showing SRHG for scattering in and out of the laser plane of polarization (in-plane: $k_z = 0$; out-of-plane: $k_y = 0$). In-plane emission at the Nth harmonic is predominantly (at the growth maxima) into a single forwards direction and $(N + 1)/2$ backwards angles when N is odd and $N/2$ backwards angles when N is even [12]. There is no exact side scattering of any harmonic in this plane. Direct backscattering occurs only at odd harmonics [16] with even harmonic emission emerging at oblique angles. Direct forwards scattering, near the fundamental only, is well approximated as a 6-mode hybrid of Raman forwards scattering and the relativistic modulational instability [13]. Forwards scattering from the peak growth points emerges for the fundamental ($N = 1$) at 27° to the forwards direction (laboratory view), at 35° when $N = 2$ and 50° when $N \geq 3$. Emission is polarized in the laser plane of polarization. Out-of-plane SRHG occurs at all angles but peaks strongly at very oblique angles when $q > 1$. The largest growth rate, $\Gamma = 0.25\Omega_0$, is for out-of-plane scattering near the fundamental at 50° to the forwards direction. This compares with the peak in-plane growth of $0.21\Omega_0$. The polarization of the out-of-plane emission alternates with the harmonic number [the electric (magnetic) field lies in the $\hat{\mathbf{y}}$ direction for N odd (even)].

Figure 2 shows the emergence of TPD at $n_{\rm cr}/4$. The low intensity theory [6] predicts that instability is maximized in the plane of polarization with peak growth along the hyperbola $K_x^2 = 4K_y^2 + 3$ (in the pulse frame). This behavior is seen in the contours of Fig. 2(a). However, this growth is overlain by an almost orthogonal pattern of SRHG showing a coincidence in the conditions for SRHG and TPD. At low intensity there can be a resonant triplet of modes with SRHG parasitic to

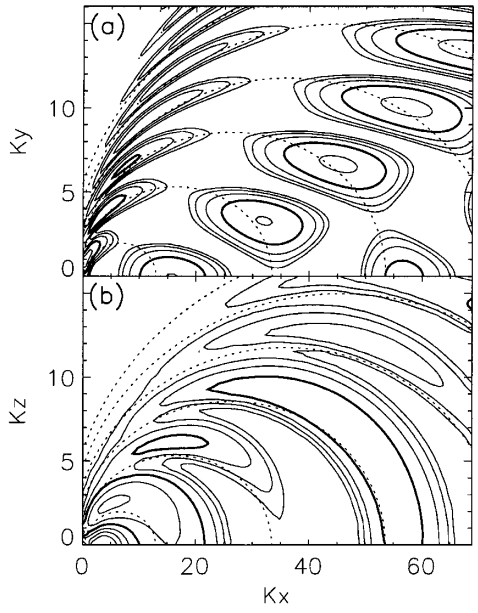

FIG. 1. Contour plot of the growth rate Γ/Ω_0 vs $\mathbf{K} = \mathbf{k}/\Omega_0$ in underdense plasma ($n_{0,\rm lab} \approx 0.1 n_{\rm cr}$) when $q = 5$ for scattering (a) in and (b) out of the laser plane of polarization. The contours displayed are 0.04(0.04)0.24. The bold contour has the growth rate 0.16.

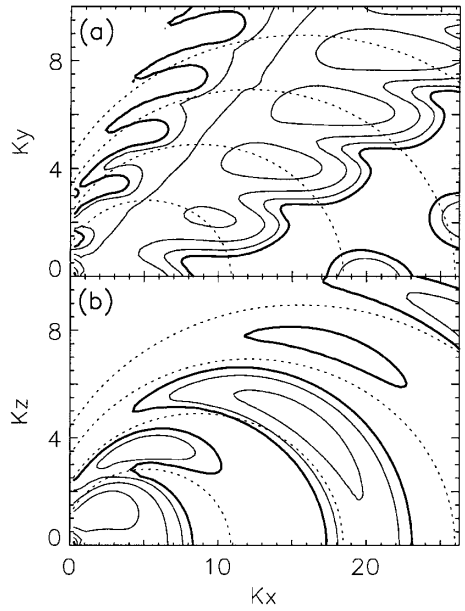

FIG. 2. Growth rate contour plot for the relativistic quarter critical density $n_{\rm cr}/4$ but otherwise as for Fig. 1. Contours plotted are 0.16(0.04)0.28.

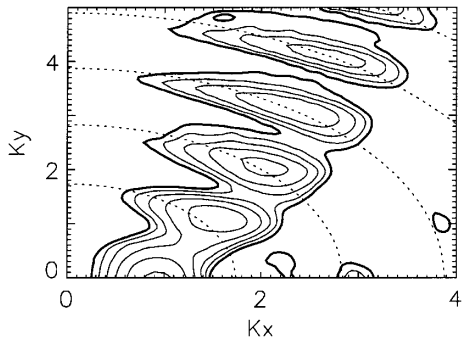

FIG. 3. Growth rate contour plot for the relativistic critical density $n_{\rm cr}$ but otherwise as for Fig. 1. Contours plotted are 0.16(0.04)0.36.

TPD. At high intensity, there is both strong SRHG and TPD coupling with emission at near half-harmonic frequencies. The out-of-plane behavior is similar to the low density case showing strong SRHG but no TPD. However, a curiosity of the out-of-plane case is that the emission is into near integer harmonics rather than at the expected half-harmonic frequencies observed for in-plane scattering.

The laser light at its cutoff ($u = 0$, $\Omega_0 = 1$, $n_{0,\rm lab} = n_{\rm cr}$) is a near transverse oscillation where p_{0y} has the shape of linked parabolas [17], $p_{0x} \approx 0$, while $v_{0y} = \pm 1$ approaches a rectangular waveform. Figure 3 shows results in the (k_x, k_y) plane only since there is symmetry about the k_y axis. Peak growth arises when SRHG is simultaneous with the occurrence of standing wave solutions (frequency spectra symmetric about zero frequency). At low intensity, the laser driver is unstable mainly to perturbations perpendicular to the laser polarization direction ($k_y = 0$). The second growth peak corresponds to the simultaneous resonance of two counterpropagating pairs of plasma waves and second harmonic light waves. At high intensity higher harmonic branches emerge, all with comparable growth rates. Their spectra consist of resonant Fourier modes at exact harmonics $\omega = \pm N$ satisfying $\omega^2 = \omega_{\rm pr}^2 + k^2$ coupled through electrostatic fluctuations at $\omega = \pm l$ where $l = 0, 1, \ldots, N$. Sinusoidal dipole drivers have been studied in weakly relativistic regimes by Tsintsadze and extended, for perturbations in the k_y direction, to fully relativistic regimes by Guérin *et al.* [18].

Equations (6)–(8) represent a general pulse-frame model describing all electron parametric instabilities amenable to a cold electron fluid description. Only kinetic regimes of instability are excluded (such as stimulated Compton scattering). We have shown that ultraintense linearly polarized laser light is very unstable to perturbations across a broad range of wave numbers. Strong filamentation and stimulated harmonic generation to high order appear at all densities up to the relativistic critical density.

[1] P. Sprangle, E. Esarey, and A. Ting, Phys. Rev. Lett. **64**, 2011 (1990).
[2] D. Umstadter *et al.,* Science **273**, 472 (1996).
[3] M. Tabak *et al.,* Phys. Plasmas **1**, 1626 (1994).
[4] T. Tajima and J. Dawson, Phys. Rev. Lett. **43**, 267 (1979).
[5] J. F. Drake *et al.,* Phys. Fluids **17**, 778 (1974).
[6] A. B. Langdon *et al.,* Phys. Rev. Lett. **43**, 133 (1979).
[7] C. J. McKinstrie and R. Bingham, Phys. Fluids B **4**, 2626 (1992).
[8] C. E. Max, Phys. Fluids **16**, 1480 (1973).
[9] B. Quesnel *et al.,* Phys. Rev. Lett. **78**, 2132 (1997); S. Guérin *et al.,* Phys. Plasmas **2**, 2807 (1995).
[10] T. M. Antonsen and P. M. Mora, Phys. Fluids B **5**, 1440 (1994); Phys. Rev. Lett. **74**, 4440 (1995).
[11] W. B. Mori *et al.,* Phys. Rev. Lett. **72**, 1482 (1994); C. D. Decker *et al.,* Phys. Plasmas **3**, 1360 (1996); **3**, 2047 (1996).
[12] A. S. Sakharov and V. I. Kirsanov, Phys. Rev. E **49**, 3274 (1994); Phys. Plasmas **4**, 3382 (1997).
[13] H. C. Barr, S. J. Berwick, and P. Mason, Phys. Rev. Lett. **81**, 2910 (1998).
[14] A. V. Borovsky *et al.,* Phys. Rev. E **59**, 2253 (1999).
[15] A. I. Akhiezer and R. V. Polovin, Sov. Phys. JETP **3**, 696 (1956).
[16] P. Sprangle and E. Esarey, Phys. Rev. Lett. **67**, 2021 (1991).
[17] C. Max and F. Perkins, Phys. Rev. Lett. **27**, 1342 (1971).
[18] N. L. Tsintsadze, Sov. Phys. JETP **32**, 684 (1971); S. Guérin, P. Mora, and G. Laval, Phys. Plasmas **5**, 376 (1998).